

Non-orthogonal Frequency Hopping Signal Underdetermined Blind Source Separation in Time-Frequency Domain

¹ Chengjie Li ¹ Lidong Zhu ² Zhen Zhang

Abstract—In this paper, a novel Matching Optimization Algorithm (*MOA*-algorithm) based on underdetermined blind source separation is proposed for non-orthogonal frequency hopping signal (that is, inner products are not always equal to zero in the same time-frequency point). Compared to traditional methods, the separation method is formulated as matching optimization. In our method, we accomplish the underdetermined blind source separation by computing the Short Time Fourier Transform (STFT) of each observation to get the signal time-frequency distribution, then we formulate the separation problem as matching optimization. In matching optimization, a new cost function is designed to improve the complete separation, and we make negative gradient direction as the steepest descent direction, to verify the proposed method on several simulations. The experimental results demonstrate the effectiveness of the proposed method.

Index Terms—Blind Source Separation, Frequency hopping signal, Time-Frequency Distribution, Cost Function, Pearsons correlation coefficient.

1 2 3

I. INTRODUCTION

Blind source separation (BSS) is a major research area in signal processing and machine learning, and is used in many fields, such as image recognition, speech enhancement, biomedical signal processing, wireless communications etc. [1][2][3]. BSS aims to extract individual components from their mixture samples where there is very limited, or no, prior information on mixture samples or the mixing process. Recently, many BSS methods are based on Independent Component Analysis with the assumption that the sources are independent signals. Some other methods based on Wigner-Ville Distribution (WVD) are proposed, but there is a contradiction between time-frequency concentration and cross-term interference in these methods [4]. At present, most traditional BSS methods assume that the source signals are statistically independent or the mixed matrix is full column rank. However, in many situations, this hypothesis is not valid. Consequently, recovering the source signals by multiplying the mixed matrix's pseudo inverse cannot be used. In practical terms, the overdetermined mixture assumption is not always satisfied, thus it is necessary to solve the problem of underdetermined blind source separation (UBSS). Compared with the

classical BSS approaches, the method in this article requires less constraints on the source signals, such as stationarity and independence. So it is more suitable to separate non-stationary sources, such as Frequency-Hopping (FH) signal.

Frequency-Hopping (FH) signal has been widely used in military field and modern communication systems due to its high security and good anti-jamming ability [5]. To meet the need of Counter-reconnaissance, *FH* signal blind source separation research has been a focus. Recently, some researchers discuss orthogonal *FH* signals underdetermined blind source separation method based on sparsity [6][7], however, non-orthogonal Frequency Hopping Signal Underdetermined Blind Source Separation is a challenge. In this article, we propose a non-orthogonal underdetermined blind source separation method based on convex optimization methods, that is, *MOA*-algorithm. The problem is described as follows: (a) By computing the Short Time Fourier Transform (STFT) of each observation, we can get the signal' time-frequency distribution. (b) We construct the cost function according to the sample data in time-frequency domain. (c) We find the optimal solution of the cost function by using the steepest descent method.

The rest of this paper is organized as follows. In Section II, we introduce the preparatory work of this article, In Section III, we introduce the blind source signal separation algorithm, that is, *MOA*-algorithm. In Section IV, we introduce and discuss the experimental results. Finally, the conclusion is drawn in Section V.

II. PREPARATORY WORK

In this section, we introduce the related preparatory work of *MOA*-algorithm.

A. BSS Model

BSS aims at separating a set of N unknown sources from a set of M observations. Usually, the observations are obtained from M sensors, each sensor receives a mixture from those sources, the framework of BSS model is as below:

The principle of BSS is shown in Fig.1. The matrix $S(t) = [s_1(t), s_2(t), \dots, s_N(t)]$ is composed of N unknown sources, and the matrix $Y(t) = [y_1(t), y_2(t), \dots, y_M(t)]^T$ represents M observations. Considering linear instantaneous mixtures model only, each observation is described as below [8]:

$$y_j(t) = \sum_{i=1}^N a_{ij}s_i(t) + n_i(t), j = 1, 2, \dots, M \quad (1)$$

¹University of Electronic Science and Technology of China, Chengdu, Sichuan, China, E-mail: junhongabc@126.com, zld@uestc.edu.cn

²NCS Pte. Ltd. of Singapore Tele-communications Limited, Ang Mo Kio Street 62, NCS Hub, Singapore, E-mail: zhangzhen@ncsi.com.cn

³Manuscript submitted on August 29, 2016

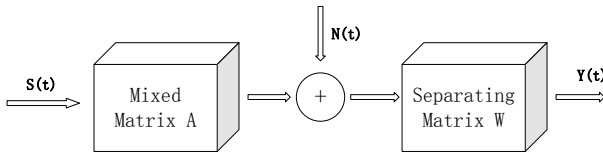
Non-orthogonal Frequency Hopping Signal Underdetermined
 Blind Source Separation in Time-Frequency Domain


Fig. 1. Framework of BSS Model

here, a_{ij} is the (i, j) th element of the mixed matrix, $n_i(t)$ is the i th component of the noise. Equation (2) can also be written in matrix form,

$$Y(t) = AS(t) + N(t) \quad (2)$$

According to the relationships among the numbers of original signal (M) and the numbers of receiving antenna (N), blind source signals can be classified into overdetermined blind separation ($M < N$), determined blind separation ($M = N$) and underdetermined blind separation ($M > N$).

B. Frequency-Hop Signal Model

The *FH* signal is a kind of non-stationary signals whose carrier frequency changes along with time, it can be expressed as [5]:

$$f(t) = \sqrt{2S} \sum_k \text{rect}_{T_H}(t - kT_H - \alpha T_H) \cdot e^{j2\pi f_k(t - kT_H - \alpha T_H) + j\theta} + n(t), 0 < t \leq L \quad (3)$$

here, L is the length of the sample data, rect_{T_H} is the rectangular window whose width equals to T_H , T_H is the hop duration, f_k is the carrier frequency of the k th hop, αT_H is hop timing, θ is the phase of the *Fh* signal, $n(t)$ is additive noise, S is the power of the signal.

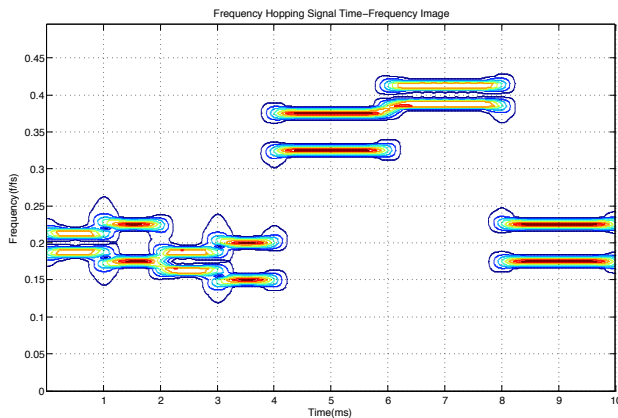


Fig. 2. Frequency Hopping Signal Time-Frequency Image

Fig.2 describes the time-frequency distribution of a *FH* signal. we can see there are five hops in this sample. The length of the whole hops is one hop duration. We can see that all hops of the *FH* signal are actually finite sine waveforms without any overlap in time domain with each other. Each of the finite sine waveforms is uniquely decided by the three

followed parameters, T_k denotes the location of k th hop in time domain, f_k denotes the location of k th hop in frequency domain, T_H denotes the length in time domain.

The problem in this paper focuses on how to separate the initial Non-orthogonal Frequency Hopping Signal without any more prior knowledge.

III. MOA-ALGORITHM

A. Problem Formulation

The mixed signals are certain to collide in the time-frequency domain when the mixed signals are non-orthogonal, as is shown in Fig.3. We can judge whether signals collide according to the number of signals in frequency domain [9]. The signals do not collide if the signal number is equal to the number of source signals in frequency domain. The signals collide if the signal number is less than the number of source signals in frequency domain. We can separate the mixed signals with Density Component Analysis Method when the source signals do not collide [10], which will be concisely introduced in the following part 3.2, and the separated signal will be signal vector space \mathcal{S}_1 . The mixed collided source signals will be the mixed signal vector space \mathcal{S}_2 . We can separate them with Matching Optimization Algorithm (*MOA*).

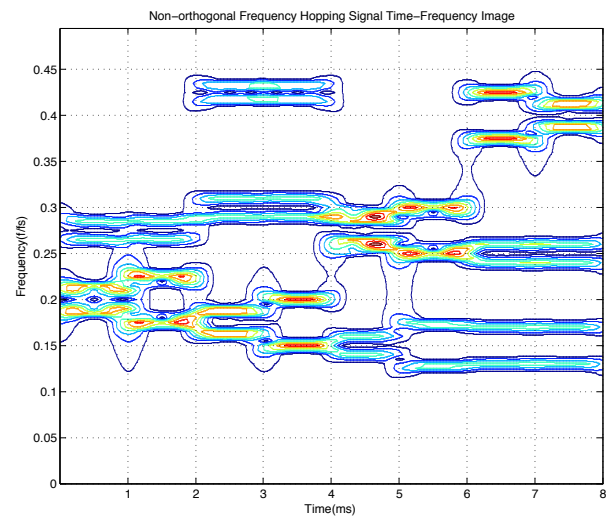


Fig. 3. Non-orthogonal Frequency Hopping Signal Time-Frequency Image

B. Density Component Analysis Method

In this section, we introduce the Density Component Analysis Method concisely, and the detailed research is another research.

(1) Construct Cost Function Pair (ρ_i, δ_i)

According to the time-frequency domain sampling points i , we compute two quantities: its local density ρ_i and its distance δ_i from points of higher density. Both quantities depend only on the distances d_{ij} between sampling data points, which are assumed to satisfy the triangular inequality. The local density ρ_i of data point i is defined as:

$$\rho_i = \sum_j \chi(d_{ij} - d_c) \quad (4)$$

in above equation, if $x < 0$ then $\chi(x) = 0$ otherwise $\chi(x) = 1$, d_c is a cutoff distance. Basically, ρ_i is the number of sampling points, the distance of sampling points to sampling point i is smaller than d_c . The algorithm is sensitive only to the relative magnitude of ρ_i in different points, that is to say, for large data sets, the results of the analysis are robust with respect to the choice of d_c .

δ_i is measured by computing the minimum distance between the sampling point i and any other sampling point with higher density:

$$\delta_i = \min_{j: \rho_j > \rho_i} (d_{ij}) \tag{5}$$

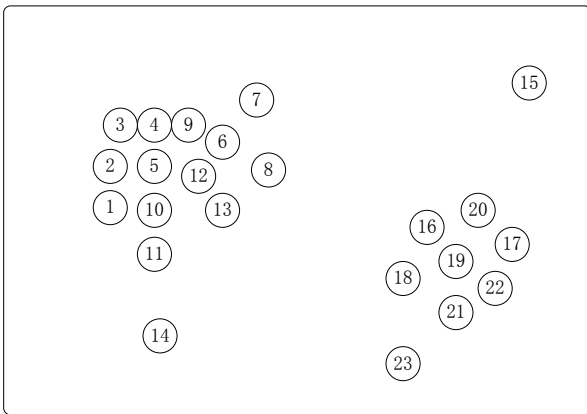


Fig. 4. Decision Coordinate System. Sampling Data Points are Ranked in Order of Decreasing Density

(2) Construct Decision Coordinate System

This observation, which is the core of the algorithm, is illustrated by the simple example in Fig.4. Fig.4 shows 23 points embedded in a two-dimensional space [25]. Based on

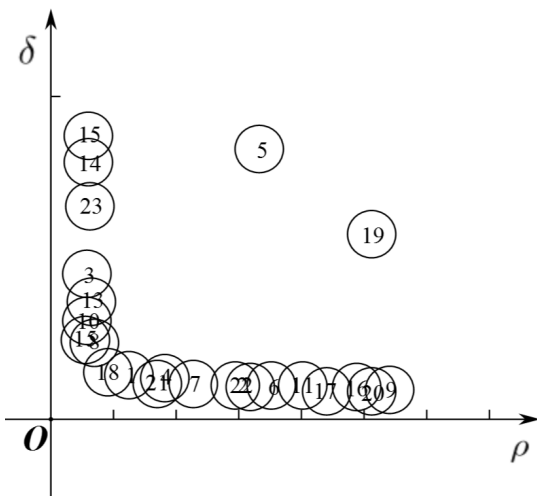


Fig. 5. Decision Coordinate System. Sampling Data Points are Ranked in Order of Decreasing Density

the distribution of the sampling points in a two-dimensional

space above, decision coordinate system can be found in Fig.5, which shows the plot of δ_i as a function of ρ_i for each sampling point. It is seen that although the data number 2 and 22 are very near, they are not the cluster center due to the small value of δ . Meanwhile, we can see from Fig.5 that data 2 and 22 belong to different centers, i.e., 5 and 19 respectively. Hence, only the data with both large values of δ and ρ will be treated as cluster center, such as data number 5 and 19 in Fig.5. Note that the points 14, 15, and 23 have a relatively high δ and a low ρ . These points are isolated data and can be considered as clusters with single point, which is also named outliers.

After the cluster centers have been found, each remaining sampling point is assigned to the same cluster as its nearest neighbor of higher density.

We can separate the mixed signals with the above Density Component Analysis Method when the source signals do not collide, and the separated signal will be signal vector space \mathcal{Y}_1 . The mixed collided source signals will be the mixed signal vector space \mathcal{Y}_2 . We can separate the mixed signal vector space \mathcal{Y}_2 with MOA-algorithm as follows.

C. Construct Cost Function of MOA-algorithm

According to the separated signal vector space \mathcal{Y}_1 and the mixed collision source signals vector space \mathcal{Y}_2 , we can construct the following cost function.

$$\min_{A,E} \|\beta - \sum \lambda_i x_i\|_p + E, \text{ subject to } x_i \in X \tag{6}$$

here, β is the collision vector, and belongs to the \mathcal{Y}_2 . λ_i is the weight coefficient of x_i . $\sum x_i$ is the random sum of x_1, x_2, \dots, x_n , $x_i \in \mathcal{Y}_1$. $A = [x_i, x(i+1), x(i+2), \dots, x(i+k)]$. E is the Mean Squared Error(MSE), here,

$$E = \sqrt{\frac{\sigma_1^2 + \sigma_2^2 + \dots + \sigma_n^2}{n}}, \tag{7}$$

$\sigma_1, \sigma_2, \dots, \sigma_n$ is the error value.

We find the optimal solution of the cost function by using the steepest descent method. So, the negative gradient direction $d = -\frac{\nabla \min(\cdot)}{\|\nabla \min(\cdot)\|}$ is the steepest descent direction [11].

IV. PERFORMANCE ANALYSIS OF MOA-ALGORITHM

A. Algorithm Process Analysis

MOA-algorithm aims at reconstructing the mixed matrix and the source signal according to $\mathcal{Y}_1, \mathcal{Y}_2$ by solving the following optimization problem:

$$\min_{A,E} \|\beta - \sum \lambda_i x_i\|_p + \sqrt{\frac{\sigma_1^2 + \sigma_2^2 + \dots + \sigma_n^2}{n}}, \tag{8}$$

subject to $x_i \in X$

where the first term penalizes non-sparse solutions, the last term is a classical data fidelity term. Because \mathcal{Y}_1 is separated signal vector space, it is sparse. The sparsity level is measured by the l_p norm of the sources. We generally choose either $p = 1$ or $p = 2$. In [12], [13], how to choose to a particular l_p norm for the sparsity penalty have been discussed in more

Non-orthogonal Frequency Hopping Signal Underdetermined
 Blind Source Separation in Time-Frequency Domain

detail. If E is fixed, the l_2 norm is particularly appealing since it makes the estimation of β be a convex optimization problem. In *MOA*-algorithm, we will choose $p = 2$ which has been shown to provide the best separation results in the following simulations in part 5. So, the problem in (8) is classically tackled by using the steepest descent method. So, the negative gradient direction $d = -\frac{\nabla \min(\cdot)}{\|\nabla \min(\cdot)\|}$ is the steepest descent direction.

According to (8), the mixed matrix A is estimated by looking for the optimal solution of the following convex problem:

$$\min_A \|\beta - \sum \lambda_i x_i\|_p + E, \quad \text{subject to } x_i \in X \quad (9)$$

The equation (9) can be decomposed into two terms: i) a non-convex p -norm penalty, and ii) a quadratic and differentiable data fidelity term E . Let $\forall x_1, x_2 \in \mathcal{B}_1$, $|E(x_1) - E(x_2)| \leq L |x_1 - x_2|$, the quadratic term E is differentiable and its gradient satisfied L -Lipschitz conditions. That shows the problem in (9) can be solved exactly by using the Forward-Backward splitting algorithm [14]. In [15], this optimization strategy has been used for solving the steepest descent method, but it has the strong weakness of dramatically increasing the computational cost of the algorithm: update A would require efficient but costly iterative algorithms. Furthermore, each time the source matrix A is updated in the algorithm *MOA* algorithm, it is fully re-estimated. Therefore, it may not be necessary to update with high precision A at each step of *MOA* algorithm.

B. Convergence of *MOA*-Algorithm

Because the problem in (8) is not convex, convergence to a critical point can be expected. For a fixed collision vector β (β belongs to the \mathcal{B}_2), minimizing the problem in (8) can be tackled by Block Coordinate Relaxation [16]. Then, this procedure can make solve sequences of convex minimization problems take place of a globally non-convex problem. In [17], convergence of block coordinate relaxation for the minimization of non-differentiable and non-convex cost functions have been proved by Tseng. According to [17], the minimization of function in (8) converges to a critical point when the parameters λ_i and x_j are fixed.

Firstly, decreasing the thresholds is a strategy to improve the robustness of the *MOA* algorithm to spurious local minima. In the field of optimization, this procedure is reminiscent of the fixed point continuation technique, which has been proposed to speed up the minimization of $\|\bullet\|_p$ -penalized least-squares [18]. The convergence of the *MOA* algorithm would be guaranteed as long as steps (8) are alternated until convergence for each value of λ_i . The thresholds are however updated at each iteration of the *MOA* algorithm, which helps speeding up the algorithm but might prevent it from convergence.

Secondly, weight coefficient λ_i is updated at each iteration, but also might prevent the *MOA* algorithm from convergence. Lastly, in the spirit of re-weighted l_1 techniques, the weight coefficients are updated based on estimating of $x_j \in \mathcal{B}_2$ [49 19]. If this strategy is a well motivated heuristic, the convergence of the *MOA* algorithm is not theoretically grounded.

In numerical experiments, in order to show better performance of the proposed algorithm, we measure the convergence speed with E_{ct} value. The results are shown in Fig.6, the horizontal axis is iteration number, the vertical axis is E_{ct} value and E_{ct} is defined as [20]:

$$E_{ct} = \sum_{i=1}^M \left(\sum_{j=1}^M \frac{|c_{ij}|}{\max_k |c_{ik}| - 1} \right) + \sum_{j=1}^M \left(\sum_{i=1}^M \frac{|c_{ij}|}{\max_k |c_{kj}| - 1} \right) \quad (10)$$

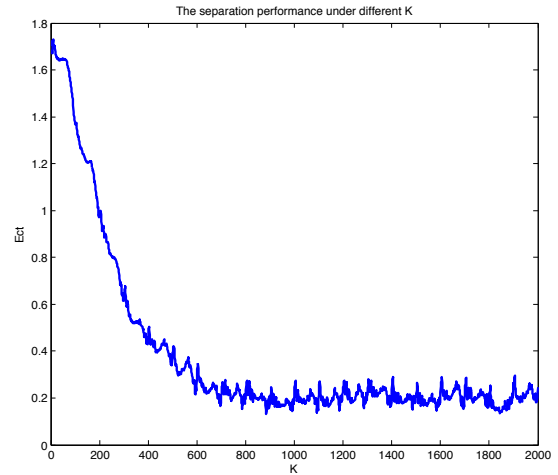


Fig. 6. Convergence Performance of the *MOA* algorithm.

From Fig.6, we can see that the algorithm has a good convergence performance, and it has a satisfied convergence speed.

C. Choosing the Parameters in *MOA*-algorithm

The *MOA* algorithm relies on a re-weighting procedure that penalizes certain entries of the estimated sources. The weights are function of the $\|\bullet\|_p$ norm of the columns of A . They somehow measure the activity of each sample across the sources. Intuitively, choosing a low value for p seems quite natural since it yields more contrast between sparse and non-sparse columns of A . This argument would make perfect sense if the true sources were known. A trade-off has to be made between the two following options [21]:

- i) Large values for p might lead to an under-penalization of less discriminant entries.
- ii) Small values for p provides a larger penalization of non-sparse entries of A , which is desirable to efficiently separate s.p.c. sources.

However, at the beginning of the *MOA* algorithm, one has only access to imperfect, if not erroneous, estimates of A . In this case, small values of p might mis-penalize/mis-favor entries of A which can eventually hamper the separation process. Alleviating this dilemma is made by starting with a high value for p -typically and then decreasing it, at each iteration, towards some final value p_f . Several values for p_f have been tested; it turns out that choosing $p_f = 0.001$ leads to a good trade-off for all the experiments we carried out. Smaller values for p_f did not bring any noticeable improvement [22].

D. Discussion About the Impact of Noise

In this section, we discuss the impact of the re-weighting scheme on the performances of the *MOA* in the noisy condition. First, in the *MOA* algorithm, the weights λ_i are estimated from the estimated sources. These sources are obtained via Step 1 of the *MOA* algorithm. In the low noise limit, one interesting feature of the proposed re-weighting scheme is that it is inversely proportional to the amplitude of the columns of A . More precisely, this entails that large entries of A which are shared by several sources are more penalized than small entries with the same relative distribution across the sources. Strongly penalizing large and correlated entries is desirable since they are detrimental to the estimation of the mixed matrix and the sources [23]. In the noisy setting, the situation turns out to be rather different since small-amplitude samples are more likely perturbed by noise than large amplitude entries. On one hand, the proposed re-weighting procedure might be disastrous for the separation of the sources whether they are partially correlated or not. Indeed, since the weights are inversely proportional to the amplitude of the columns of the sources, the proposed procedure will tend to favor small entries which are more affected by the presence of noise. On the other hand, Step 1 of the *MOA* algorithm rejects entries with amplitudes smaller than some prescribed noise-dependent level. This should lower the impact of noise on the performances of the *MOA* algorithm [24].

In [18 25], the authors demonstrated that the *MOA* algorithm is robust to additive noise contamination. This is especially true whenever morphological diversity holds; in that case the most discriminant sources are the entries of the sources with the most significant amplitudes. It turns out these entries are also the least contaminated by additive noise. In the case of s.p.c. sources, the most discriminant sources are not necessarily the large-amplitude samples. A first consequence is that noise will be very likely to have a strong impact on the quality of the separation.

V. SIMULATION AND BLIND SOURCE SIGNAL SEPARATION RESULTS

In this section, we present computer simulations, in order to illustrate the performance of the proposed *MOA*-algorithm. In the simulation, the non-orthogonal frequency hopping signal in time-frequency domain will be separated from the mixed signals.

Each parameter is defined as follows: $fb = 2 * 10^5 Hz$ for sample rate, $Rb = 10^3 bps$ for transmission bit rate, $v = 500 hop/s$ for hopping speed, $f_0 = 2 * 10^3 Hz$ for modulation frequency, $m = 8$ for bit numbers, the original signal numbers as $MK = 3$, and the receiving antenna numbers as $RK = 2$.

The sent source signal's Time-Frequency images are shown in the Fig.7. We aim to separate each object signal from the received mixed signals.

After Gauss channel transitions, the received mixed signal Time-Frequency images are shown in Fig.8 (Received Composite Signal). Here, we consider two channels to fully simulate the realistic signal transmission, which are shown from top row to the bottom row in Fig.8, respectively.

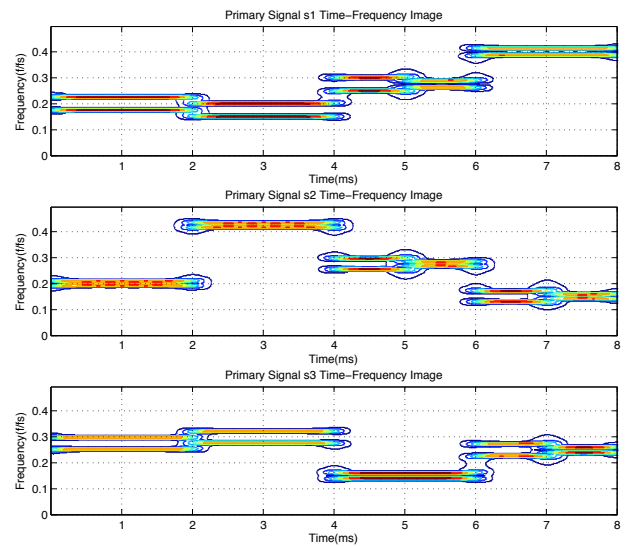


Fig. 7. The sent source signals waveforms. Three sent source signals are considered.

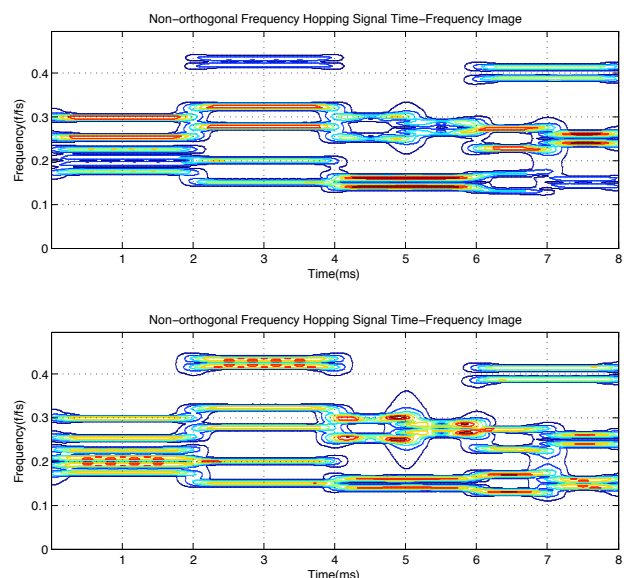


Fig. 8. The Received Mixed Signal Waves after Gaussian Channels. Two Gaussian Channels are considered.

A. The First Comparative Experiment of Effect

By using the proposed *MOA*-algorithm, the final blind source separation waveforms are shown in Fig.9, where three signals are displayed. It is seen that the obtained three object signals are very similar to the initial object signals in Fig.7.

We compare the signals between Fig.7 and Fig.9 by objective evaluation and further compare the separation performance with the classical searching and averaging method in frequency domain (SAMFD) [26], the Pearsons correlation coefficient value is used [27]. The results are shown in Fig.10, where

Non-orthogonal Frequency Hopping Signal Underdetermined Blind Source Separation in Time-Frequency Domain

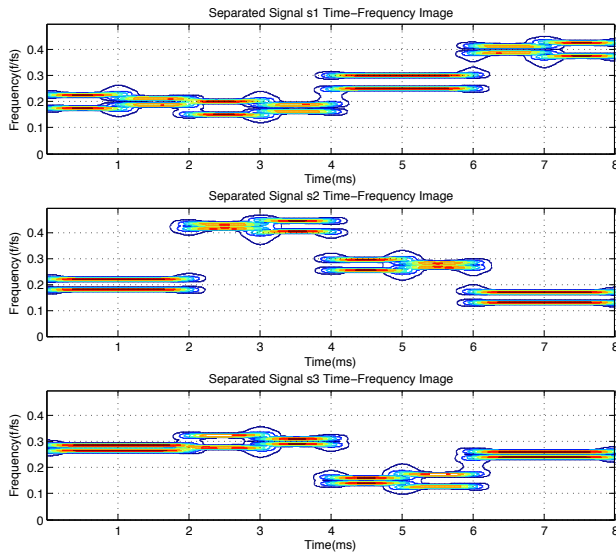


Fig. 9. Blind Source Separation Waveform Using the Proposed *MOA*-algorithm

Pearsons correlation coefficient is defined as:

$$r = \frac{\sum_{i=1}^n (x_i - \bar{x})(y_i - \bar{y})}{\sqrt{\sum_{i=1}^n (x_i - \bar{x})^2 \sum_{i=1}^n (y_i - \bar{y})^2}} \quad (11)$$

From Fig.10, we can see that blind sources signals can be efficiently separated by the *MOA*-algorithm, and it has a better performance than the classical *SAMFD*.

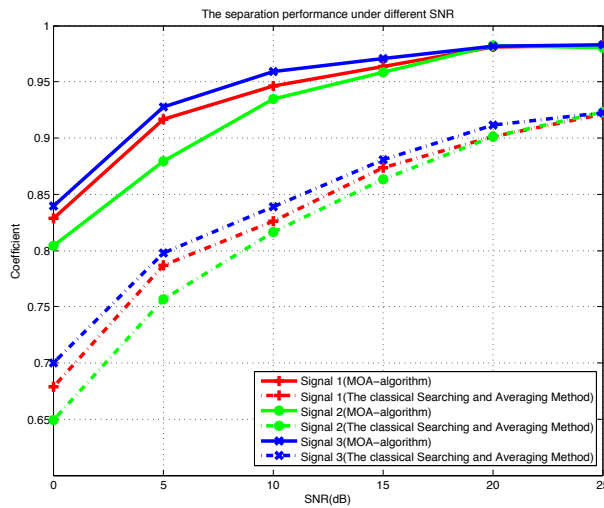


Fig. 10. Blind Source Separation Result, this article method has a better performance than classical Searching and Averaging Method

B. The Second Comparative Experiment of Effect

From the above section, we can know the *MOA*-algorithm has a satisfying separation effect. In the following section,

we will analyse the separation effect by using the error performance analysis as another evaluation criterion. In the error performance analysis, we further compare the separation performance with the classical Based on the Ratio Matrix Clustering Algorithm [28], where the *PI* value is used [29]. The formula is defined as:

$$PI = E\left\{\frac{\|A\| - \|\hat{A}\|}{\|A\|}\right\}, \quad (12)$$

here A is the mixed matrix, \hat{A} is the mixed estimation matrix. From Fig.11, we can see that blind sources signals can be

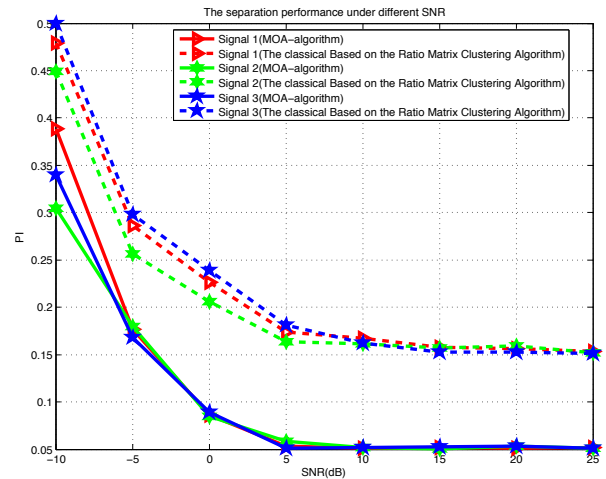


Fig. 11. Blind Source Separation Result, this article method has a better performance than classical Based on the Ratio Matrix Clustering Algorithm

efficiently separated by the *MOA*-algorithm, and it has a better performance than the classical Based on the Ratio Matrix Clustering Algorithm.

VI. CONCLUSION

In this paper, we propose non-orthogonal frequency hopping signal underdetermined blind source signal separation. Firstly, we introduce the relevant knowledge about blind source separation. Secondly, we design a novel *MOA*-algorithm to separate the mixed non-orthogonal *FH* signals. The experiment results demonstrate the effectiveness of the proposed method.

ACKNOWLEDGMENT

This work is fully supported by a grant from the national High Technology Research and development Program of China (863 Program) (No.2012AA01A502), and National Natural Science Foundation of China (No.61179006), and Science and Technology Support Program of Sichuan Province (No.2014GZX0004).

REFERENCES

- [1] Ondrej Tichy and Vaclav Smidl, Bayesian Blind Separation and Deconvolution of Dynamic Image Sequences Using Sparsity Priors, *IEEE Transactions on Medical Imaging*, Vol.34, No.1, Jan.2015, pp.258-266.

[2] Matt Atcheson, Ingrid Jafari, Roberto Togneri, Sven Nordholm, on The Use of Contextual Time-Frequency Information for Full-Band Clustering-Based Convolutional Blind Source Separation, IEEE International Conference on Acoustic, Speech and Signal Processing (ICASSP), pp.2114-2118.

[3] Leonardo T. Duarte, Joao M.T.Romano, Senior Member, Christian Jutten, Karin Y. Chumbimuni-Torres, and Lauro T. Kubota, Application of Blind Source Separation Methods to Ion-Selective Electrode Arrays in Flow-Injection Analysis, IEEE Sensors Journal, Vol.14, No.7, July.2014, pp.2228-2229.

[4] Belouchrani A, Abed-Meraim K, Cardoso JF, et al., A blind source separation technique using second order statistics, IEEE Transactions on Signal Processing, Vol.45, No.2, 1997, pp.434-444.

[5] Zhi-Chao Sha, Zhi-Tao Huang, Yi-Yu Zhou, Feng-Hua Wang, Frequency-hopping signals sorting based on underdetermined blind source separation, IET Communications, 2013, Vol.7, Iss.14, pp.1456-1464.

[6] Jerome Bobin, Jeremy Rapin, Anthony Larue, and Jean-Luc Starck, Sparsity and Adaptivity for the Blind Separation of Partially Correlated Sources, IEEE Transactions on Signal Processing, Vol.63, No.5, March 1, 2015.

[7] Sun Long Wang, Wei Chen, Ning Hua Zhu, Jian Guo Liu, Wen Ting Wang, Jin Jin Gu, A Novel Optical Frequency-Hopping Scheme for Secure WDM Optical Communications, IEEE Photonics Journal. Frequency-Hop Scheme for WDM Communications, Vol.7, No.3, June 2015.

[8] Fangyuan Nan, SVD reconstruction algorithm and determination of signal number by frequency domain information, Antennas and Propagation Society International Symposium, vol.1, 1995,pp.428-430.

[9] Mohamed Anis Lohmari, Mohamed Saber Naceur, and Mohamed Rached Boussema, A New Sparse Source Separation-Based Classification Approach, IEEE Transactions on Geoscience and Remote Sensing, Vol.52, No.11, November 2014, pp.6924-6936.

[10] DIMITRI P. BERTSEKAS, On the Goldstein-Levitin-Polyak Gradient Projection Method, IEEE Transactions on Automatic Control, Vol.21, No.2, April 1976,pp.174-183.

[11] Arvind Ganesh, Zihan Zhou, Yi Ma, Separation of A Subspace-Sparse Signal: Algorithms And Conditions, IEEE International Conference on ICASSP 2009, pp.3141-3144.

[12] J.Bobin, J.L.Starck, M.J.Fadili, and Y.Moudden, Sparsity and morphological diversity in blind source separation, IEEE Trans. Image Process., Vol.16, No.11, pp.2662-2674, 2007.

[13] J.Bobin, J.L.Starck, Y.Moudden, and M.J.Fadili, Blind source separation:The sparsity revolution, Adv. Imag. Electron Phys., Vol.152, pp. 221-306, 2008.

[14] P.L.Combettes and V.R.Wajs, Signal recovery by proximal forward-backward splitting, SIAM J. Multiscale Model. Simulat., Vol.4, No.4, pp.1168-1200, 2005.

[15] Bernard Widrow, J.Mccool, A comparison of adaptive algorithms based on the methods of steepest descent and random search, IEEE Transactions on Antennas and Propagation, September 1976, pp.615-637

[16] A.Bruce, S.Sardy, and P.Tseng, Block coordinate relaxation methods for nonparametric signal de-noising, in Proc. SPIE-The Int. Soc. for Opt. Eng., 1998, Vol.3391, pp.75-86.

[17] Paul Tseng, A coordinate gradient descent method for nonsmooth separable minimization, Mathematical Programming, March 2009, Volume 117, Issue 1, pp.387C423.

[18] Wotao Yin, Stanley Osher, Donald Goldfarb, and Jerome Darbon, Bregman Iterative Algorithms for ℓ_1 -Minimization with Applications to Compressed Sensing, SIAM Journal on Imaging Sciences, Volume 1, Issue 1, pp.143C168.

[19] E.J.Candes, M.B.Wakin, and S.P.Boyd, Enhancing sparsity by reweighted l_1 minimization, Journal Fourier Anal. Appl., Vol.14, pp.877C905, 2007.

[20] Bin Li,Ruogu Li., and Atilla Eryilmaz, On the Optimal Convergence Speed of Wireless Scheduling for Fair Resource Allocation, IEEE/ACM Transactions on Networking, Vol. 23, No. 2, April 2015, pp.631-643.

[21] Jerome Bobin, Jeremy Rapin, Anthony Larue, and Jean-Luc Starck, Sparsity and Adaptivity for the Blind Separation of Partially Correlated Sources, IEEE Transactions on Signal Processing, Vol.63, No.5, March 1, 2015, pp.1199-1213.

[22] John Canny, Computational Approach to Edge Detection, IEEE Transactions on Pattern Analysis and Machine Intelligence, Vol. PAMI-8, No. 6, November 1986, pp.679-698.

[23] Emmanuel J. Candes, Justin Romberg, and Terence Tao, Robust Uncertainty Principles: Exact Signal Reconstruction From Highly Incomplete Frequency Information, IEEE Transactions on Information Theory, Vol. 52, No. 2, February 2006, pp.489-509.

[24] Irina F. Gorodnitsky, and Bhaskar D. Rao, Sparse Signal Reconstruction from Limited Data Using FOCUSS: A Re-weighted Minimum Norm

Algorithm, IEEE Transactions on Signal Processing, Vol.45, No.3, March 1997, pp.600-616.

[25] J. Bobin, J. L. Starck, M. J. Fadili, and Y.Moudden, Sparsity and Morphological Diversity In Blind Source Separation, IEEE Trans. Image Process. Vol.16, No. 11, 2007, pp.2662C2674.

[26] Olivier Meste, Herve Rix, Pere Caminal, and Nitish V. Thakor, Ventricular Late Potentials Characterization in Time Frequency Domain by Means of a Wavelet Transform, IEEE Transactions on Biomedical Engineering, Vol. 41, No. 7, July 1994, pp.625-634.

[27] S. M. Hassan Hosseini, Mehdi Vakilian, and Gevork B. Gharehpetian, Comparison of Transformer Detailed Models for Fast and Very Fast Transient Studies, IEEE Transactions on Power Delivery, Vol. 23, No. 2, April 2008, pp.733-741.

[28] Tao Xiang, and Shaogang Gong, Video Behavior Profiling for Anomaly Detection, IEEE Transactions on Pattern Analysis and Machine Intelligence, Vol. 30, No. 5, May 2008, pp.893-908.

[29] Nikolaos P. Papanikolopoulos, Pradeep K. Khosla, and Takeo Kanade, Visual Tracking of a Moving Target by a Camera Mounted on a Robot: A Combination of Control and Vision, IEEE Transactions on Robotics and Automation. Vol.9, No.1, February 1993, pp.14-35.



Chengjie Li received the B.Sc. degree in Shandong normal University, Qufu(Confucius hometown), China, 2004, the M.Sc. degree in applied mathematics in Xihua University, Chengdu, China, 2010. Now Chengjie Li is studying for Ph.D. degree in Communication and Information System in University of Electronic Science and Technology of China (UESTC), Chengdu, China, 2013.



Lidong Zhu received the B.S and M.S from Sichuan University, Chengdu, China, in 1990 and 1999, respectively, and the Ph.D. degree in Communication and Information Systems from Electronic Science and Technology of China, Chengdu, China, in 2003. From July, 2009 to June 2010, he was a visiting scholar with Department of electronic engineering of The University of Hong Kong. His research interests include satellite communications, blind source separation, and communication countermeasure.



Zhen Zhang received the B.Sc. degree in Sichuan University, 2005. Received the M.Sc degree in Xihua University, 2010. Now Zhen Zhang is working in NCS. Her research interests include channel code, signal processing, and intelligent information processing.